

# Raman Spectroscopy Analysis of the Morphology of Gold Nanoparticles Produced by Laser Ablation in Aqueous Proteinogenic Amino Acid for the Detection of Mercury in Water

Hipólito Carbajal-Morán<sup>1\*</sup>

<sup>1</sup> Instituto de Investigación de Ciencias de Ingeniería, Facultad de Ingeniería Electrónica-Sistemas, Universidad Nacional de Huancavelica, Jr. La Mar 755, Pampas 09156, Huancavelica, Perú

\* Corresponding author's e-mail: [hipolito.carbajal@unh.edu.pe](mailto:hipolito.carbajal@unh.edu.pe)

## ABSTRACT

The objective of the research was to analyze by Raman spectroscopy the morphology of gold nanoparticles generated by laser ablation in L-Cysteine of purity  $\geq 97\%$  dissolved in ultrapure water for the detection by color change of mercury dissolved in water. Three samples of 10 ml of ultrapure water were prepared with aggregation of 10  $\mu$ l of L-Cysteine with concentrations of 1, 10 and 20 mM; the generation of the gold nanoparticles was by laser ablation with a wavelength  $\lambda = 1064$  nm, energy of 60.28 mJ/p located at 30 cm from the convex lens generating ablation at 10 cm on a gold plate of dimensions 10 $\times$ 15 mm with thickness of 1 mm, for 30 min. The gold nanoparticles generated in these aqueous environments were characterized by Raman spectroscopy using a laser with a sensitivity of 785 nm with Raman Shift analysis range 860–3200  $\text{cm}^{-1}$  and controlled power at 499 mW. The nanoparticles presented maximum peak resonance around Raman Shift 1164.96  $\text{cm}^{-1}$  and 1288.06  $\text{cm}^{-1}$ . With the AuNPs + L-Cysteine sample with concentration of 10 mM, the author proceeded to the detection of  $\text{Hg}^{2+}$  prepared in 20  $\mu$ l of ultrapure water at concentrations of 0.1, 5 and 10  $\mu$ M; when adding 100  $\mu$ l of AuNPs + L-Cysteine two peak absorbance spectra were obtained with different amplitudes observed by UV-Vis spectroscopy, indicating that  $\text{Hg}^{2+}$  decreased the repulsion of the negatively charged AuNPs, generating the visible color change for the three concentrations of  $\text{Hg}^{2+}$  with 25 minutes of agitation, turning intense purple for 10  $\mu$ M of  $\text{Hg}^{2+}$ ; enabling the detection of mercury in water.

**Keywords:** Raman spectroscopy, AuNPs, laser radiation, polluted water, mercury.

## INTRODUCTION

Nanoscience is concerned with investigating the phenomena and manipulation of materials at the nanometer level, while nanotechnology focuses on the design, characterization and application of complex structures, devices and systems by controlling the properties, shape and size of matter at the nanometer scale (Shih et al., 2020; Zhu et al., 2021). These two emerging disciplines possess a significant multidisciplinary approach and are of great importance from both scientific and technological points of view (Kumar et al., 2023).

Metal nanoparticles are produced under two main approaches: bottom-up and top-down. In the bottom-up approach, techniques such as sol-gel,

molecular condensation, vapor deposition, electrochemistry and chemistry are used to synthesize the nanoparticles (Jamkhande et al., 2019). On the other hand, in the top-down approach, techniques such as chemical etching, mechanical, optical, thermal, and sputtering processes are employed to produce nanoscale structures from larger structures by removing material and creating templates with varied shapes (Chow et al., 2019; Slepíčka et al., 2019). This approach is used in the fabrication of various materials in industries such as semiconductors (Kumar et al., 2021). On the other hand, the bottom-up approach is a simpler and cheaper method, and is used to build inorganic and organic materials into defined structures, at the molecular level and atom by atom, which

finds applications in many biological processes. However, a disadvantage of this approach is that it is currently not possible to fabricate integrated devices that are complex, as self-assembly is only mastered in relatively simple nanostructured materials (Khan, 2020).

Metallic nanoparticles composed of noble metals, such as gold (Au) and silver (Ag), are the most appreciated and arouse great interest from researchers, due to their ability to interact with light through surface plasmon resonance (Hammami & Alabdallah, 2021; Vasudevan et al., 2022). Gold nanoparticles (AuNPs) constitute a material with high potential to be used as building blocks for plasmonic and other optical devices (Hano & Abbasi, 2021). Gold nanoparticles have been employed in various applications in fields such as chemistry (Bayda et al., 2019), material sciences, physics, medicine, life sciences and environmental sciences (Saravanan et al., 2021).

AuNPs have been synthesized using a variety of physicochemical and biological processes, which have had significant impact on the environment. These nanoparticles are of particular importance due to their extensive history of environmental applications. On the other hand, pulsed laser ablation in liquid (PLAL) is playing an increasingly important role as a methodology for the fabrication of nanostructures without the need for chemicals and stabilizers (Al-Kinani et al., 2021; Choudhury et al., 2022). Various nanomaterials have been obtained and PLAL engineering is gaining significant relevance to promote this approach in the production of nanostructures (Sarfraz & Khan, 2021). The distinctive, advanced and enhanced characteristics of gold nanoparticles in colloidal state largely depend on the stabilization of the nanoparticles. The surface must be functionalized considering the distance between the particles, as well as their size and morphology (Carbajal-Morán et al., 2022), which can be controlled by laser power and wavelength (Torrisi et al., 2018).

The protein amino acid as L-Cysteine is a molecular agent capable of working with metal nanoparticles especially with AuNPs in controlled concentrations, making it a compound capable of detecting ionic heavy metals in water, presenting changes in the visible color spectrum (Khamcharoen et al., 2022), so this element was used in the work.

The mercury ion ( $\text{Hg}^{2+}$ ) is considered a global pollutant that has a negative impact on the health

of people exposed to this substance (Yang et al., 2020). Its most serious effects are related to damage to the nervous system, making it a public health problem that requires appropriate attention especially in children (Barone et al., 2021). Mercury can enter the body through food and water intake (Aveiga et al., 2022), as well as inhalation and absorption, making exposed populations (Lensoni et al., 2023), such as those involved in activities like small-scale mining, especially vulnerable and requiring strategies to mitigate exposure (Budianta et al., 2020). Among the most common and stable forms of mercury contamination is the water-soluble divalent ion,  $\text{Hg}^{2+}$ , which implies that environmental monitoring of  $\text{Hg}^{2+}$  in the aqueous state is necessary and is a demanding task; the detection and quantification of metal ions is crucial for environmental and domestic monitoring, the food industry and clinical diagnosis (Vardè et al., 2022). Therefore, it is necessary to implement mechanisms to detect mercury in water and food sources to prevent serious effects on human health.

This work addresses the production of gold nanoparticles generated by laser ablation in aqueous medium containing L-Cysteine in different concentrations with dispersion in water, for the detection of  $\text{Hg}^{2+}$  through color changes indicating its concentration in a visible way.

## MATERIALS AND METHODS

Gold nanoparticles were generated with the Nd: Yag Q-Smart 450 pulsed laser device with low divergent output beam and allowing ablation applications, presenting timing signals for pulsing in automatic mode of 6 ns (Quantel, 2019) as seen in Figure 1. The FWHM pulse width is variable and is exploited for the generation of metal nanoparticles. In this work with a laser pulse duration set at 116  $\mu\text{s}$ , AuNPs were produced at a rate of two pulses per second for wavelengths of 1064 nm with energy of 450 mJ/p and 532 nm with energy of 220 mJ/p, generating AuNPs for 30 and 60 minutes. The target location was a 10×15 mm gold plate at a distance of 10 cm from the focus of the convex lens for 532/1064 nm.

AuNPs were generated for 30 minutes in 10 ml ultrapure water in three quartz cuvettes to which 10  $\mu\text{l}$  of L-Cysteine  $\geq 97\%$  purity with concentrations of 1, 5 and 10 mM, respectively were added for each cuvette, functionalizing the

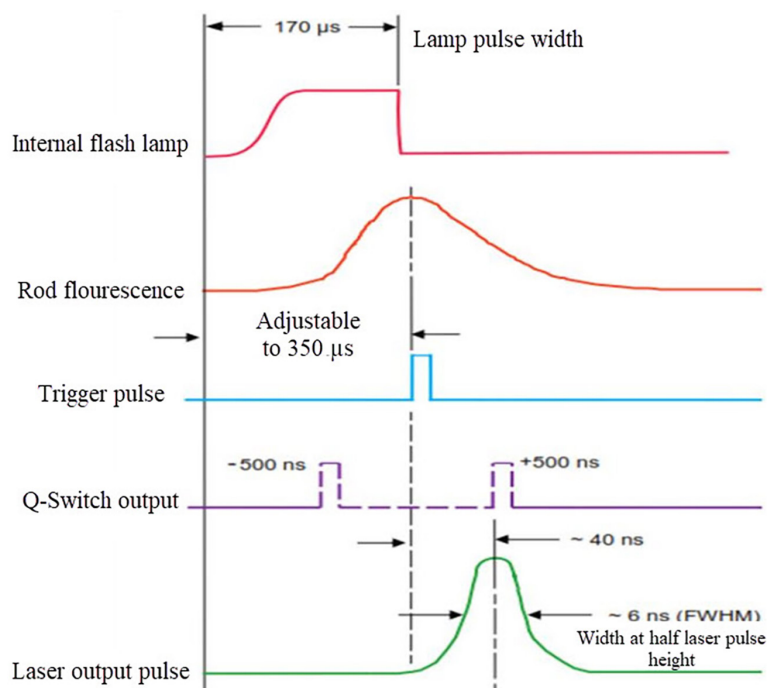


**Figure 1.** Timing signals in automatic mode, internal flash lamp and internal Q-Switch

gold nanoparticles during the process of their production with the previously configured ablation laser (see Figure 2). Subsequently, the solutions were shaken and centrifuged for one hour at room temperature, then dispersed in ultrapure water for experimental application.

The L-Cysteine functionalized AuNPs samples were characterized with the Raman spectroscopy base AvaSpec-ULS2048CL-EVO-RS set for (788–1100 nm), with FC-PC connector via USB port (Avantes, 2020). This spectroscopy generates a 765 nm laser, which is delivered by an integrated ultra-high-performance fiber optic cable. This device includes an integrated wavelength-stabilized laser source with Raman filter packages, beam generation optics and high efficiency Raman spectra collection optics (See Figure 3).

Using the AvaSoft software from Avantes (2018), the signals were sampled every 2 ms. The process of characterizing the samples started with directing the Raman tester towards the sample contained in the quartz cuvette; subsequently, these signals are interpreted by the ICCD spectrometer and sent to the AvaSoft software interface with the active Raman utility. In this interface, the relationship between the absorption of the spectra (arbitrary units) and their corresponding Raman Shift ( $\text{cm}^{-1}$ ) is graphically defined, which allowed to determining the morphology of the AuNPs produced and functionalized with L-Cysteine.

## RESULTS AND DISCUSSION

With the molecule L-Cysteine  $\geq 97\%$  purity, the Raman spectrum of which is presented in Figure 4, different concentrations were prepared to be added to 10 ml of ultrapure water, achieving functionalized AuNPs in 30 min in the samples containing 10 μl of L-Cysteine with concentrations of 1, 10 and 20 mM.

For each aggregation of 10 μL of L-Cysteine in ultrapure water, the author proceeded with laser ablation on the Au metal plate immersed in L-Cysteine:  $\text{H}_2\text{O}$  for 30 min, a higher Raman intensity was obtained as a result for the 10 mM concentration of L-Cysteine (1166.94, 1029.27), as shown in Figure 5; the three main Raman spectra of the samples are located at 1166.94  $\text{cm}^{-1}$ . For the 20 nM concentration of L-Cysteine the intensity decreases with respect to the previous one and another Raman spectrum appears (1155.06, 446.33), indicating a deformation of the nanoparticle upon functionalization (Seth, 2020).

The functionalized nanoparticles were subjected to centrifugation for separation and then dispersed by agitation forming a colloid for colorimetric detection of the analyte constituted by  $\text{Hg}^{2+}$ .

The color change detection process of  $\text{Hg}^{2+}$  in aqueous state was carried out at room temperature. Solutions of 0.1 μM, 5 μM and 10 μM of  $\text{Hg}^{2+}$  were prepared in 20 μl of ultrapure

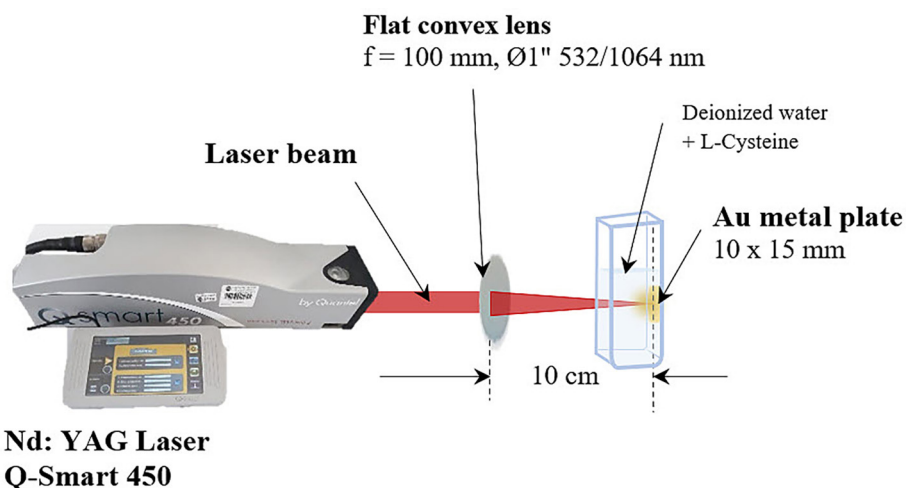


Figure 2. Installation of the Nd: Yag laser equipment for the production of AuNPs + L-Cysteine

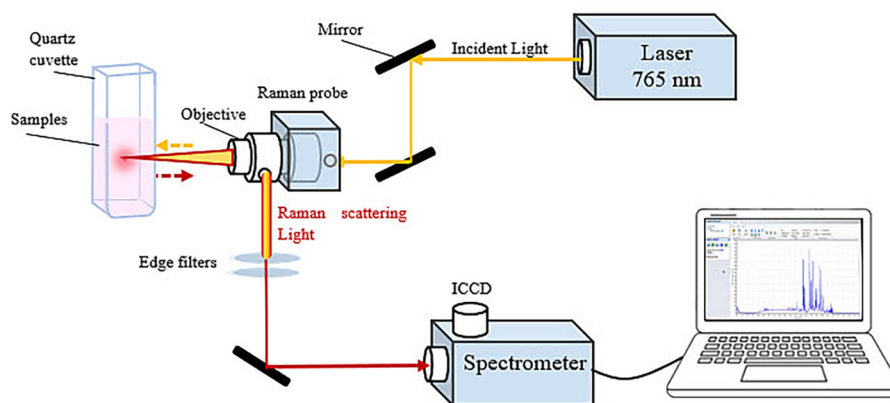


Figure 3. Raman spectroscopy setup for characterization of AuNPs + L-Cysteine

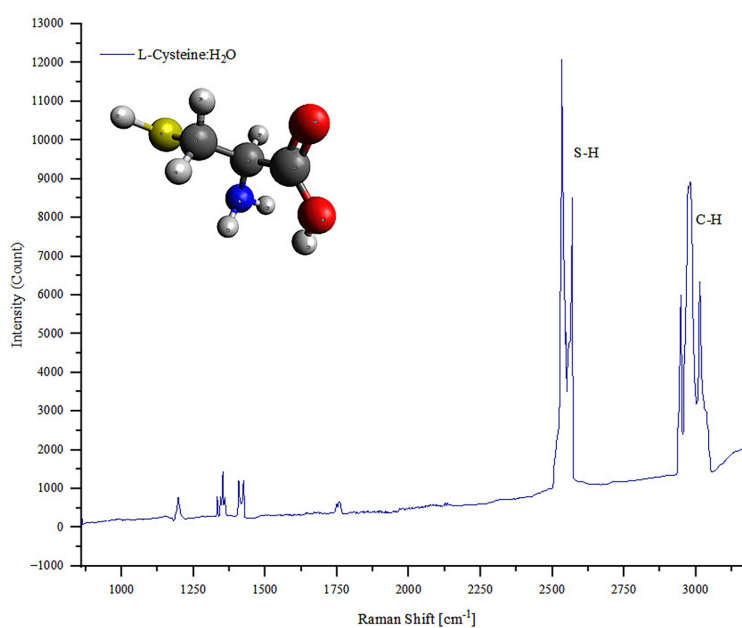
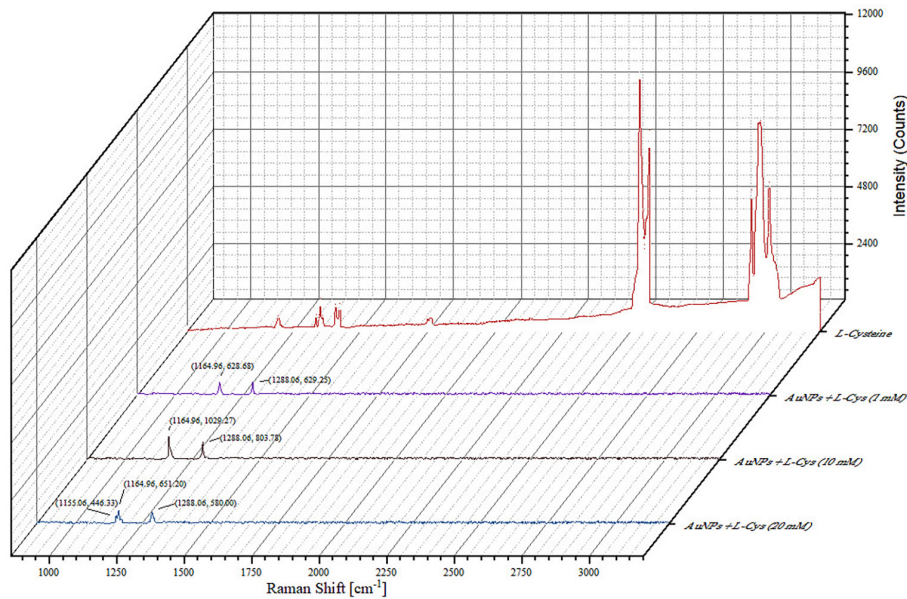


Figure 4. Raman spectrum of L-Cysteine  $\geq 97\%$  in  $\text{H}_2\text{O}$



**Figure 5.** Raman spectra of AuNPs generated and functionalized on L-Cysteine with concentrations of 1 mM, 10 mM and 20 mM

water, since these concentrations are significant for this type of application (Annadhasan et al., 2014; Darbha et al., 2008), to which 100  $\mu\text{l}$  of AuNPs functionalized with L-Cysteine were added, obtaining the absorbance spectra in Figure 6.

The absorbance spectra were measured by UV-Vis spectroscopy, the AuNPs + L-Cysteine (10 mM) presents a maximum absorbance amplitude of 0.61 with wavelength of 524.31 nm being this the basis on which the different samples

were generated by  $\text{Hg}^{2+}$  aggregation; upon addition of 0.1  $\mu\text{M}$  of  $\text{Hg}^{2+}$  it was possible to detect an absorbance level of 0.08 for an approximate wavelength of 715 nm, this wavelength is the same for the different aggregations of  $\text{Hg}^{2+}$ , upon aggregation of 5  $\mu\text{M}$  of  $\text{Hg}^{2+}$ , an absorbance level of 0.20 was obtained and for aggregation of 10  $\mu\text{M}$  of  $\text{Hg}^{2+}$ , an absorbance level of 0.25 was found. The absorbance peaks near wavelength 715 nm for each sample correspond to the binding of AuNPs + L-Cysteine with  $\text{Hg}^{2+}$ .

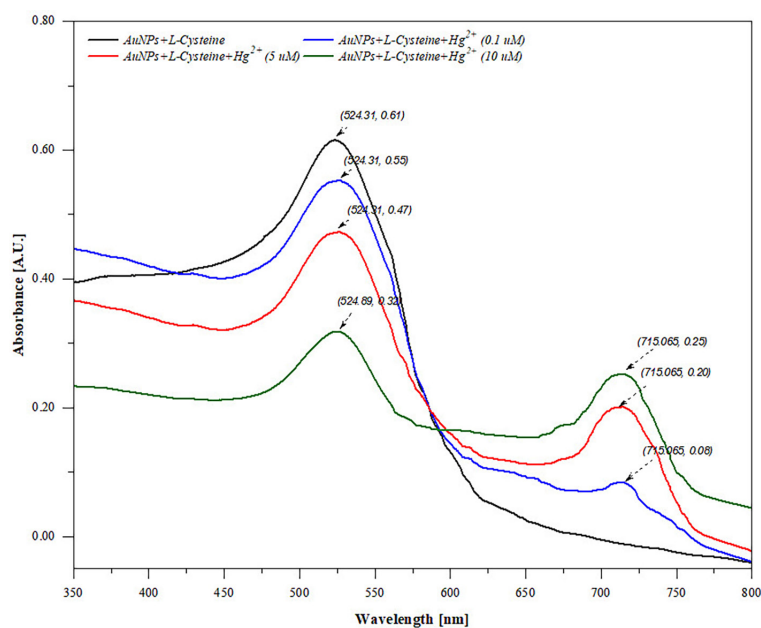


**Figure 6.** UV-Vis absorbance spectra generated by AuNPs + L-Cysteine with addition of 0.1, 5 and 10  $\mu\text{M}$  of  $\text{Hg}^{2+}$



**Figure 7.** Colorimetric detection of different concentrations of  $\text{Hg}^{2+}$  (0.1, 5 and 10  $\mu\text{M}$ )

The detection of  $\text{Hg}^{2+}$  in the aqueous state decreases the repulsion of the negatively charged AuNPs, so it generates a visible color change after 25 minutes, allowing the visual detection of the presence of this element, starting from the aggregation of 0.1  $\mu\text{M}$  of  $\text{Hg}^{2+}$ , the color variation for the aggregation of 10  $\mu\text{M}$  of  $\text{Hg}^{2+}$  being more noticeable, as seen in Figure 7, which agrees with the studies of Seth (2020).

## CONCLUSIONS

Raman spectroscopy allowed the analysis of the morphology of gold nanoparticles produced by laser ablation of  $\lambda = 1064$  nm with an energy of 60.28 mJ/p in an aqueous environment of 10 ml ultrapure water functionalizing at the same time in the presence of three samples with 10  $\mu\text{l}$  of the amino acid L-Cysteine  $\geq 97\%$  at concentrations of 1, 10 and 20 mM, presenting a more defined spectrum in the sample with concentration of 10 mM, being the spectra of higher intensity in Raman Shift 1164.96  $\text{cm}^{-1}$  and 1288.06  $\text{cm}^{-1}$ .

With the sample of AuNPs + L-Cysteine with 10 mM concentration, the author proceeded to the detection of  $\text{Hg}^{2+}$  prepared in 20  $\mu\text{l}$  of ultrapure water at concentrations of 0.1, 5 and 10  $\mu\text{M}$  by adding 100  $\mu\text{l}$  of AuNPs + L-Cysteine two peak absorbance spectra with different amplitudes were obtained, indicating that  $\text{Hg}^{2+}$  decreased the repulsion of negatively charged AuNPs, generating the visible color change for the three concentrations of  $\text{Hg}^{2+}$  with 25 min of stirring. The use of gold nanoparticles generated and functionalized with proteinogenic amino acids is an important option for the detection of ionic agents, such as  $\text{Hg}^{2+}$ .

## Acknowledgements

This work was made possible thanks to funding from the Universidad Nacional de

Huancavelica through the Fondo de Desarrollo Socioeconómico de Camisea (FOCAM).

## REFERENCES

1. Al-Kinani, M.A., Haider, A.J., Al-Musawi, S. 2021. Design and synthesis of nanoencapsulation with a new formulation of Fe@ Au-CS-CU-FA NPs by pulsed laser ablation in liquid (PLAL) method in breast cancer therapy: in vitro and in vivo. *Plasmonics*, 16(4), 1107–1117. <https://doi.org/10.1007/s11468-021-01371-3>
2. Annadhasan, M., Muthukumarasamyvel, T., Sankar Babu, V.R., Rajendiran, N. 2014. Green Synthesized Silver and Gold Nanoparticles for Colorimetric Detection of  $\text{Hg}^{2+}$ ,  $\text{Pb}^{2+}$ , and  $\text{Mn}^{2+}$  in Aqueous Medium. *ACS Sustainable Chemistry & Engineering*, 2(4), 887–896. <https://doi.org/10.1021/sc400500z>
3. Avantes. 2018. Espectrómetro UV-Vis-NIR – AvaSpec-ULS2048x64-EVO. <https://www.medicaexpo.com/prod/avantes/product-104219-950813.html>
4. Avantes. 2020. AvaRaman Bundles. <https://www.avantes.com/products/raman/avaraman-bundles/>
5. Aveiga, A., Pinargote, C., Peñarrieta, F., Teca, J., Alcántara, F. 2022. Adsorption of Mercury and Zinc in Agricultural Soils by *Sphagneticola trilobata*. *Journal of Ecological Engineering*, 23(3), 230–235. <https://doi.org/10.12911/22998993/146115>
6. Barone, G., Storelli, A., Meleleo, D., Dambrosio, A., Garofalo, R., Busco, A., Storelli, M.M. 2021. Levels of mercury, methylmercury and selenium in fish: Insights into children food safety. *Toxics*, 9(2), 39. <https://doi.org/10.3390/toxics9020039>
7. Bayda, S., Adeel, M., Tuccinardi, T., Cordani, M., Rizzolio, F. 2019. The history of nanoscience and nanotechnology: from chemical–physical applications to nanomedicine. *Molecules*, 25(1), 112. <https://doi.org/10.3390/molecules25010112>
8. Budianta, W., Ardiana, A., Andriyani, N.D., Fahmi, F.L. 2020. Impact of mercury contamination by artisanal mining on soil and the use of natural zeolite for stabilization. *IOP Conference Series: Earth and Environmental Science*, 479(1), 12020. <https://doi.org/10.1088/1755-1315/479/1/012020>

9. Carbajal-Morán, H., Rivera-Esteban, J.M., Aldama-Reyna, C.W., Mejía-Uriarte, E.V. 2022. Functionalization of Gold Nanoparticles for the Detection of Heavy Metals in Contaminated Water Samples in the Province of Tayacaja. *Journal of Ecological Engineering*, 23(9), 88–99. <https://doi.org/10.12911/22998993/151745>
10. Choudhury, K., Srivastava, A., Singh, R.K., Kumar, A. 2022. Laser-produced plasma: Fabrication of size-controlled metallic nanoparticles. In *Plasma at the Nanoscale* (pp. 37–61). Elsevier. <https://doi.org/10.1016/B978-0-323-89930-7.00005-4>
11. Chow, T.H., Li, N., Bai, X., Zhuo, X., Shao, L., Wang, J. 2019. Gold nanobipyramids: An emerging and versatile type of plasmonic nanoparticles. *Accounts of Chemical Research*, 52(8), 2136–2146. <https://doi.org/10.1021/acs.accounts.9b00230>
12. Darbha, G.K., Singh, A.K., Rai, U.S., Yu, E., Yu, H., Chandra Ray, P. 2008. Selective Detection of Mercury (II) Ion Using Nonlinear Optical Properties of Gold Nanoparticles. *Journal of the American Chemical Society*, 130(25), 8038–8043. <https://doi.org/10.1021/ja801412b>
13. Hammami, I., Alabdallah, N.M. 2021. Gold nanoparticles: Synthesis properties and applications. *Journal of King Saud University-Science*, 33(7), 101560. <https://doi.org/10.1016/j.jksus.2021.101560>
14. Hano, C., Abbasi, B.H. 2021. Plant-based green synthesis of nanoparticles: Production, characterization and applications. In *Biomolecules*. MDPI, 12(1), 31. <https://doi.org/10.3390/biom12010031>
15. Jamkhande, P.G., Ghule, N.W., Bamer, A.H., Kalaskar, M.G. 2019. Metal nanoparticles synthesis: An overview on methods of preparation, advantages and disadvantages, and applications. *Journal of Drug Delivery Science and Technology*, 53, 101174. <https://doi.org/10.1016/j.jddst.2019.101174>
16. Khamcharoen, W., Henry, C.S., Siangproh, W. 2022. A novel L-cysteine sensor using in-situ electropolymerization of L-cysteine: Potential to simple and selective detection. *Talanta*, 237, 122983. <https://doi.org/10.1016/j.talanta.2021.122983>
17. Khan, F.A. 2020. Nanomaterials: types, classifications, and sources. *Applications of Nanomaterials in Human Health*, 1–13. [https://doi.org/10.1007/978-981-15-4802-4\\_1](https://doi.org/10.1007/978-981-15-4802-4_1)
18. Kumar, R., Kumar, M., Chohan, J.S. 2021. The role of additive manufacturing for biomedical applications: A critical review. *Journal of Manufacturing Processes*, 64, 828–850. <https://doi.org/10.1016/j.jmpro.2021.02.022>
19. Kumar, R., Kumar, M., Luthra, G. 2023. Fundamental approaches and applications of nanotechnology: A mini review. *Materials Today: Proceedings*. <https://doi.org/10.1016/j.matpr.2022.12.172>
20. Lenoni, L., Adlim, M., Kamil, H., Karma, T., Suhendrayatna, S. 2023. Identification and Correlation Test of Mercury Levels in Community Urine at Traditional Gold Processing Locations. *Journal of Ecological Engineering*, 24(3), 357–365. <https://doi.org/10.12911/22998993/159062>
21. Quantel. 2019. Q-smart 450 Pulsed Nd:YAG Laser, 213 to 1064nm, 8 to 450mJ, Product – Photonic Solutions, UK. <https://www.photonicsolutions.co.uk/product-detail.php?prod=6345>
22. Saravanan, A., Kumar, P.S., Karishma, S., Vo, D.-V.N., Jeevanantham, S., Yaashikaa, P.R., George, C.S. 2021. A review on biosynthesis of metal nanoparticles and its environmental applications. *Chemosphere*, 264, 128580. <https://doi.org/10.1016/j.chemosphere.2020.128580>
23. Sarfraz, N., Khan, I. 2021. Plasmonic gold nanoparticles (AuNPs): properties, synthesis and their advanced energy, environmental and biomedical applications. *Chemistry—An Asian Journal*, 16(7), 720–742. <https://doi.org/10.1002/asia.202001202>
24. Seth, R. 2020. L-cysteine functionalized gold nanoparticles as a colorimetric sensor for ultrasensitive detection of toxic metal ion cadmium. *Materials Today: Proceedings*, 24, 2375–2382. <https://doi.org/10.1016/j.matpr.2020.03.767>
25. Shih, C.-Y., Shugaev, M.V, Wu, C., Zhigilei, L.V. 2020. The effect of pulse duration on nanoparticle generation in pulsed laser ablation in liquids: insights from large-scale atomistic simulations. *Physical Chemistry Chemical Physics*, 22(13), 7077–7099. <https://doi.org/10.1039/D0CP00608D>
26. Slepíčka, P., Slepíčková Kasálková, N., Siegel, J., Kolská, Z., Švorčík, V. 2019. Methods of gold and silver nanoparticles preparation. *Materials*, 13(1), 1. <https://doi.org/10.3390/ma13010001>
27. Torrisi, L., Cutroneo, M., Silipigni, L., Barreca, F., Fazio, B., Restuccia, N., Kovacik, L. 2018. Gold nanoparticles produced by laser ablation in water and in graphene oxide suspension. *Philosophical Magazine*, 98(24), 2205–2220. <https://doi.org/10.1080/14786435.2018.1478147>
28. Vardè, M., Barbante, C., Barbaro, E., Becherini, F., Bonasoni, P., Busetto, M., Calzolari, F., Cozzi, G., Cristofanelli, P., Dallo, F. 2022. Characterization of atmospheric total gaseous mercury at a remote high-elevation site (Col Margherita Observatory, 2543 m asl) in the Italian Alps. *Atmospheric Environment*, 271, 118917. <https://doi.org/10.1016/j.atmosenv.2021.118917>
29. Vasudevan, A., Shvalya, V., Košiček, M., Zavašnik, J., Jurov, A., Santhosh, N.M., Zidanšek, A., Cvelbar, U. 2022. From faceted nanoparticles to nanostructured thin film by plasma-jet redox reaction of ionic gold. *Journal of Alloys and Compounds*, 928, 167155. <https://doi.org/10.1016/j.jallcom.2022.167155>
30. Yang, L., Zhang, Y., Wang, F., Luo, Z., Guo, S., Strähle, U. 2020. Toxicity of mercury: Molecular evidence. *Chemosphere*, 245, 125586. <https://doi.org/10.1016/j.chemosphere.2019.125586>
31. Zhu, S., Meng, H., Gu, Z., Zhao, Y. 2021. Research trend of nanoscience and nanotechnology—A bibliometric analysis of *Nano Today*. *Nano Today*, 39, 101233. <https://doi.org/10.1016/j.nantod.2021.101233>